



PCCP

A Practical Way to Enhance the Synthesis of N₈- from an N₃-Precursor, Studied by Both Computational and Experimental Methods

Journal:	<i>Physical Chemistry Chemical Physics</i>
Manuscript ID	CP-ART-11-2020-006053.R2
Article Type:	Paper
Date Submitted by the Author:	18-Mar-2021
Complete List of Authors:	Alzaim, Safa; New Jersey Institute of Technology, Department of chemical and materials engineering Wu, Zhiyi; New Jersey Institute of Technology, Department of chemical and materials engineering Benchafia, El mostafa; New Jersey Institute of Technology, Department of Physics Young, Joshua; New Jersey Institute of Technology, Department of chemical and materials engineering wang, xianqin; New Jersey Institute of Technology, Department of chemical and materials engineering

SCHOLARONE™
Manuscripts

A Practical Way to Enhance the Synthesis of N_8^- from an N_3^- Precursor, Studied by Both Computational and Experimental Methods

Safa Alzaim, Zhiyi Wu, Mostafa Benchafia , Joshua Young,* Xianqin Wang*

Dept. of Chemical and Materials Engineering, New Jersey Institute of Technology, Newark, NJ, 07102, USA

Corresponding author: jyoung@njit.edu; xianqin.wang@njit.edu

Keywords

Polymeric nitrogen

Synthesis

Mechanism

Enhancement

DFT

Abstract

Polymeric nitrogen (PN) is a general family of materials containing all-nitrogen molecules or clusters. Although it is rare and challenging to synthesize PN members, they are attracting increasing scientific attention due to their high energy storage capacity and possible use as a green catalyst. A few theoretical calculations predicted the possible PN phases from N_2 gas, but they all require extremely high pressure and temperature to synthesize. In this work, a practical way to synthesize N_8 polymeric nitrogen from N_3^- precursor is elucidated using density functional theory calculations. The detailed mechanism, $4N_3^- \rightarrow 4N_3^* \rightarrow 2N_6 \rightarrow N_{12} \rightarrow N_{10} + N_2 \rightarrow N_8 \text{ (ZEZ)} + 2N_2$, is determined. The calculated energy barriers indicate the first step ($4N_3^- \rightarrow 4N_3^*$) is the rate-limiting step. The result guides us to rationally synthesize N_8 under UV (254nm) irradiation, chosen based on the calculated absorption spectrum for the azide anion. As expected, UV enhances N_8 yield by nearly four times. This provides an interesting route to scalable synthesis of high energy density N_8 compounds.

1. Introduction

Atmospheric nitrogen (N_2) is a diatomic molecule consisting of an extremely strong N-N triple bond. With a bond energy of 954 kJ/mol, it is one of the strongest bonds in nature ^{1 2}. Moreover, there is a very large difference in energy between this bond and the nitrogen single bond (160 kJ/mol) and double bond (418 kJ/mol). ² The five outermost valence electrons of nitrogen enables network, layer and chain structures; the chains of polymeric nitrogen (PN) are of particular interest for their energy storage capacity. ² The high stability of N_2 in comparison to PN accounts for the high energy release upon the conversion of PN to N_2 , and the high energy storage within a polymer chain of single bonds. These properties make these PN compounds high energy-density materials, with an energy density about three times that of TNT. ² Further, decomposition to nitrogen gas does not harm the environment. ¹ The high energy-density is advantageous in propellants or explosives, ³ but all of these characteristics, from the ability to form many different configurations to catalytic properties, make PN appealing in applications from energy storage to catalysis⁴.

Unfortunately, transforming N_2 to stable PN compounds requires enormous temperature and pressure, and the compounds are then only stable in extreme conditions. Many experiments have produced various phases of PN, at high temperature and pressure conditions ⁵⁶⁷. However, these temperatures and pressures are not practical for scalability.

In recent years *ab initio* techniques have been utilized to find more efficient, effective and practical ways of synthesizing PN chains. In particular, the aforementioned problems with extreme conditions are one reason that computational methods are gaining increasing attention. In 2008, H Abou-Rachid *et al.* used *ab initio* methods to predict that armchair EZE N_8 within carbon nanotubes (CNT) would be stable in ambient conditions. ⁸ In 2009, Ji *et al.* found the formation energy and transition state from N_2 for this N_8 in CNT. ⁹ Also in 2009, Timoshevski *et al.* found through *ab initio* methods that armchair N_8 on a graphene substrate would be stable in ambient conditions. ¹⁰ In 2018, S Niu *et al.* computed the ambient stability of a 3D graphene/PN/graphene crystal system.² These studies demonstrated the contribution of the substrate to PN stability at ambient conditions.

In 2014, B Hirshberg *et al.* predicted through computational methods that coupled zigzag EEE and EZE N_8 would be stable at ambient conditions. ¹¹ In 2018, Battaglia *et al.* ¹² calculated the dissociation energies for both N_8 EEE and EZE isomers (as defined in Reference ¹³) to $N_6 +$

N_2 and $2N_3 + N_2$. They noted that the EEE isomer had a lower interaction energy and was geometrically more linear. This geometry would make the N_8 more capable of confinement in a CNT without distortion, and so steric effects might dictate mechanism pathways.

Another route to produce PN is through photolysis of azide to produce radical N_3^* . This approach was studied by Barat *et al.*¹⁴ and Treinin *et al.*¹⁵ in 1969 as well as Hayon *et al.*¹⁶ in 1970. They identified the absorption spectra associated with the N_3^* formation from N_3 . In 2016, Peiris *et al.*¹⁷ explored the photolysis of polynitride materials at 4.8 to 8.1 GPa of pressure. On the other hand, an experiment by Holtgrewe *et al.*¹⁸ used photochemistry to synthesize polynitrides at high pressure; however, their products were not clearly identified. This potential route to PN compounds still remains relatively unexplored.

However, in 2014, Wu *et al.*¹⁹ successfully synthesized N_8^- under ambient conditions and found it to be a highly active oxygen reduction reaction (ORR) catalyst.¹⁹ Unlike conventional PN fabrications, which used N_2 precursors in diamond-anvil cell systems, the group used an azide precursor. The azide precursor meant obviating the high temperature and pressure required to change the bonding in N_2 . The azide was subjected to cyclic voltammetry, in which a potential was swept and the resulting current measured. The process was performed in ambient conditions and produced stable N_8 PN chains, both with and without a substrate. Although the yield without a substrate is low, the finding was significant because conventional synthesis requires extreme temperature and pressure. However, the synthesis mechanism of $N_3^- \rightarrow N_3^* \rightarrow N_8$ remains unclear. In this work, density functional theory (DFT) calculations are used to determine the probable pathway for the production of EZE N_8 from azide in ambient conditions.

2. Methods

All calculations were performed using ORCA²⁰ quantum chemistry software. The input was prepared manually, with initial configurations constructed in the Avogadro package. All geometries were optimized with DFT, utilizing the B3LYP²¹ functional and aug-ss-pVDZ²² basis set, as exemplified by Bartlett¹³. A D3BJ²⁵ dispersion correction was employed. For comparison, tests were also performed with the def2-TZVPP²³ basis set, as well as with using a DLPNO-CCSD(T) coupled cluster²⁴ approach, also with a def2 basis set. All systems were fully relaxed with an SCF convergence tolerance of 10^{-9} and optimization criteria of $\Delta E = 10^{-6}$. Activation barriers were computed through surface scans of saddle-point optimizations. Vibrational

frequencies were analyzed through transition state optimizations with exact Hessian, recalculated every five steps. NEB calculations proceeded with xtb²⁶ binding and the vpo²⁷ algorithm of optimization. Lastly, a time-dependent DFT (TD-DFT) calculation was used to analyze excited states: the TD-DFT was carried out with 150 transitions and Davidson-expansion space 300. Visualizations were carried out on Chemcraft²⁸ quantum chemistry software. We also compared this with the CAM-B3LYP functional.

Experimentally, a 254 nm mercury lamp (UVP R-52g, power 100 W) was used for an investigation of the UV effect. The lamp illuminated the cyclic voltammetry synthesis process, as detailed previously¹⁹. For comparison, a 365 nm mercury lamp (UVP B-100AR, power 100W) was also used. Temperature-programmed desorption (TPD) was used to measure the PN yield. Fourier transform infrared (FTIR) and Raman spectroscopy were used to confirm the PN synthesis.

Raman spectroscopy was performed with a Thermo Scientific DXR Raman microscope. FTIR was carried out using a Nicolet ThermoElectron FTIR spectrometer combined with a MIRacle ATR platform assembly and a ZnSe plate, and denoted as ATR-FTIR. TPD was carried out using the AutoChem II 2920 system. Samples were heated in flowing helium from room temperature to 850 °C at a heating rate of 10 °C /min. The released species were monitored with an on-line mass spectrometer (QMS 200, Stanford Research Systems).

3. Results and discussion

A full geometric optimization of an azide radical (N_3^*) and anion (N_3^-) were first investigated (Fig. 1a). The Gibbs free energy of the azide anion is lower than the azide radical by 60 kcal/mol. Two azide radical molecules were then optimized in a variety of configurations to form an N_6 PN molecule. In each case, the system converged to the configuration in Fig 1b. A numerical frequency calculation then confirmed that N_6 is a stable intermediate (Supplemental Table 1). This configuration is in agreement with the lowest-energy N_6 found by Greschner *et al.*²⁹. Following this, two N_6 molecules were combined into a variety of configurations to form an N_{12} molecule. Only two of these configurations are stable, while all others decompose. Of these two, the lowest energy N_{12} configuration adopted a zigzag configuration (Fig 1c); the transition state (TS1) is shown in Figure 2a. The barrier for the formation of N_{12} from two N_6 species through TS1 is 20 kcal/mol. For comparison, the total energy difference is 19 kcal/mol with DLPNO-CCSD(T) couple cluster theory.

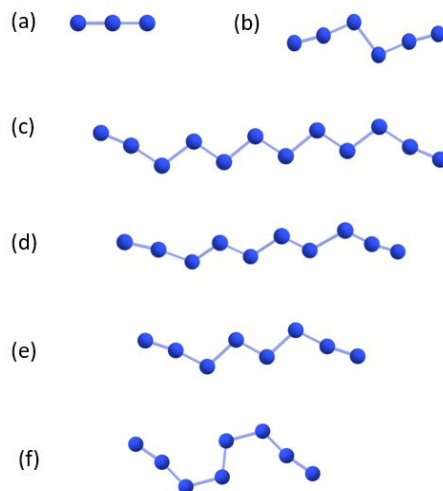


Fig. 1: Lowest energy structures of a) N_3^* , b) N_6 , c) N_{12} , d) N_{10} , e) EEE N_8 , and f) ZEZ N_8 .

A number of possible pathways from N_{12} to N_8 were then examined. In agreement with a DFT study by Battaglia *et al.*¹², N_5 was found to be unstable, decomposing into $N_3 + N_2$. Thus, it was necessary to discard any pathway based on N_5 , such as $N_{12} \rightarrow N_9 + N_3 \rightarrow N_7 + N_2 + N_3 \rightarrow N_5 + 2N_2 + N_3 \rightarrow \dots N_8$. Similarly, any pathway that builds on N_2 as a reactant was discarded, as diatomic nitrogen is inert under atmosphere condition¹. Additionally, N_4 was found to decompose to N_2 except in square or chain configurations; however, as neither of these configurations will react to form N_8 , any pathway based on N_4 was also discarded. Moreover, N_6 will not spontaneously form $N_4 + N_2$, as, again, the linear N_4 from this process was found to be highly unstable. Additionally, the possibility of sequential N_3 addition via the pathway $4N_3 \rightarrow N_6 + 2N_3 \rightarrow N_9 + N_3 \rightarrow N_{12} \rightarrow N_{10} + N_2 \rightarrow N_8 + 2N_2$ was considered, but this barrier was higher than that of N_6 to N_{12} directly. Thus, $2N_6 \rightarrow N_{12}$ is preferred pathway. Lastly, any pathway using monatomic nitrogen was excluded.

The remaining two possibilities are to transform from N_{12} to N_8 directly, or to $N_{10} + N_2$ and then to $N_8 + 2N_2$. To clarify either pathways, a saddle point optimization was carried out with relaxed scan to find the minimum energy path to the transition state, in an eigenvector-following calculation²⁰. As N_{12} dissociating into $N_{10} + N_2$ has a much lower energy barrier (5 kcal/mol) compared to the direct decomposition of N_{12} to $N_8 + 2N_2$ (60 kcal/mol barrier), it is the probable synthesis mechanism. Fig 1d and 1e show the optimized N_{10} configuration and the resulting N_8 configuration, respectively. Finally, this neutral N_8 molecule will reconfigure to N_8^- (Fig. 1f) upon reduction; N_8^- in this configuration is lower in energy than the corresponding N_8 by 32 kcal/mol.

Compared to the EEE N_8 cleaved from N_{10} , the ZEZ configuration contains one shifted atom, as seen in Fig 1d. From a nudged elastic band (NEB) calculation, it is found that this reconfiguration is nearly spontaneous with an energy barrier of only 3 kcal/mol (Supplemental Fig 3).

To determine the full synthesis mechanism, a saddle point was optimized with relaxed scan for each step leading to N_8 in order to determine the transition states. The vibrational frequencies for each step were calculated numerically; for stability, the intermediates must have no negative vibrational frequencies, while transition states exhibit one negative frequency. From N_3 to N_6 , the scan consisted of decreasing the distance between two N_3 molecules (specifically atom N1 and N6, Supplemental Figure 1) from 3 Å to 1 Å. It was found that the formation of N_6 from $2N_3$ is spontaneous.

Similarly, the N_{12} scan consisted of decreasing the distance between two N_6 molecules from 3 Å to 1 Å. From the scan, the transition state was identified (TS1, Fig. 2a); an optimization and subsequent numerical frequency calculation showed only one negative frequency, confirming this to be the transition state between N_6 and N_{12} (Supplemental Table 1). As mentioned previously, the process from N_6 to N_{12} requires overcoming the TS1 barrier with an activation energy of 20 kcal/mol. Similarly, the transition state from the decomposition of N_{12} to N_{10} (TS2) was identified and is shown in Fig. 2b. Again, an optimization and numerical frequency calculation confirm this transition state (Supplemental Table 1). From N_{12} to N_{10} , the activation barrier is about 10 kcal/mol. Finally, from N_{10} to N_8 , the transition state (TS3, Fig. 2c) energy barrier is about 15 kcal/mol. These values are relatively low and can easily be overcome by the cyclic voltammetry process. It is likely that plasma methods of fabrication would provide even more energy input, rendering these two activation barriers moot. The last step is the reduction and reconfiguration of N_8 to N_8^- . The Gibbs free energy reaction diagram for the entire aforementioned synthesis mechanism, from the azide radical to N_8^- , is shown in Fig. 3. The radicalization of azide does not require a conformational change, and so the difference in the single point energies indicates the radicalization energy, about 60 kcal/mol. As this quantity is the highest in the mechanism, it is the rate-limiting step. Finally, to demonstrate that the predictions were independent of the basis set choice, a TZVPP basis set was first used to compare with aug-ss-pVDZ. The TZVPP set has extended polarizability functions, which can be useful in analyzing the negative charge of N_8^- . Additionally, coupled cluster theory calculations were carried out; due to the high computational cost, the single-point energies rather than free energies were determined. As shown in

Supplementary Figure 5, the energy differences are very similar, confirming the validity of the calculated pathway.

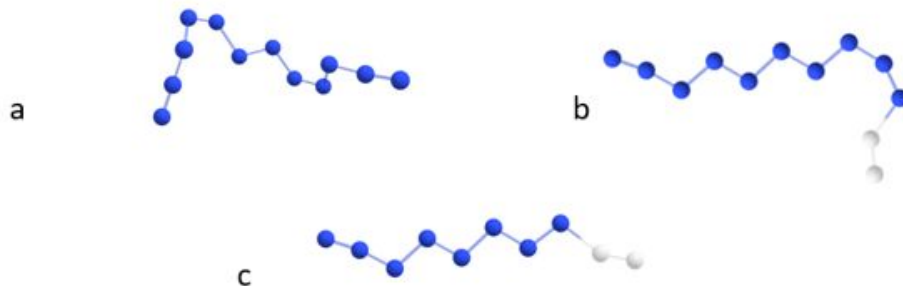


Fig. 2: a) Transition state between N_6 and N_{12} (TS 1). b) Transition state between N_{12} and N_{10} (TS 2). c) Transition state between N_{10} and N_8 (TS 3). Dissociating N atoms are shown in gray.

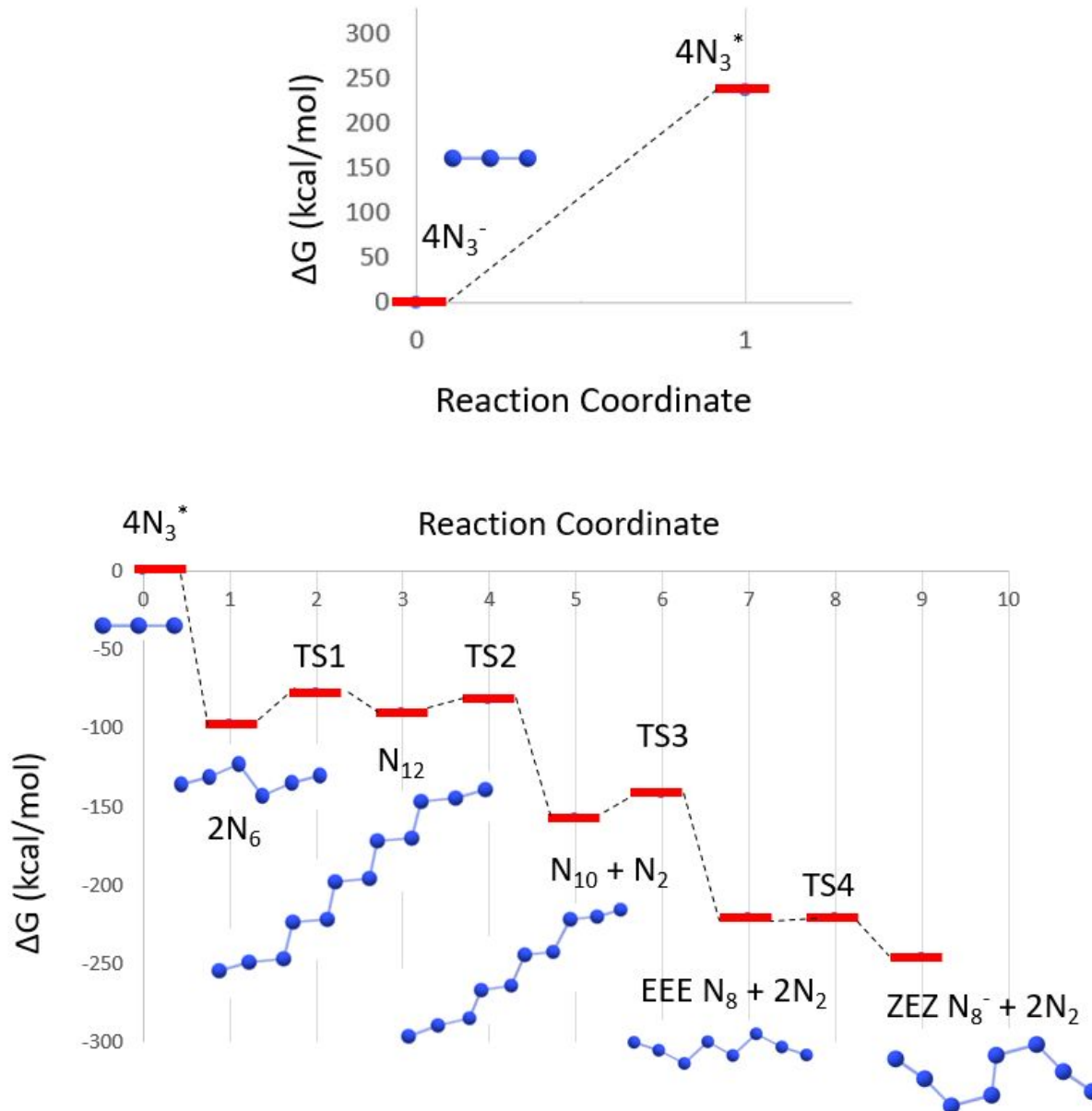


Fig. 3: a) Reaction diagram N_3^- to N_3^* . b) Reaction diagram for the synthesis mechanism of N_8^- from N_3^* .

Based on the above mechanism, the rate-limiting step of the whole mechanism, N_3^- to N_3^* with its 60 kcal/mol energy barrier, controls the yield of PN synthesis. Thus, increasing the rate of N_3^- to N_3^* would enhance the yield of PN product. A time-dependent DFT (TD-DFT) calculation

was performed on the azide ion to analyze the excitation states in this rate-limiting step. The calculated UV spectrum shows peaks at 150, 233 and 290 nm (Fig. 4). The calculation was repeated with CAM-B3LYP, showing a peak at 257 nm. This prediction indicates that exposing the azide to radiation of about 254 nm would likely enhance the conversion of N_3^- to N_3^* , as this value is within the curve of the calculated peaks, and nearly exactly at the peak in the CAM-B3LYP calculation. To confirm this, PN was synthesized following the same cyclic voltammetry (CV) procedure as the work from Wu *et al.*,¹⁹ but under UV irradiation with a wavelength of 254 nm within the absorption band. For comparison, the PN synthesis was also carried out under 365 nm light, which would not be adsorbed according to the TD-DFT calculations. The quantity of PN was determined with TPD measurements, and the yield increases by about four times under UV irradiation, as shown in Table 1. In comparison, the amount of sample from 365 nm UV light irradiation does not increase, but instead decreases slightly due to the thermal effect. The result demonstrates that UV illumination combined with CV is a promising way to produce this PN species.

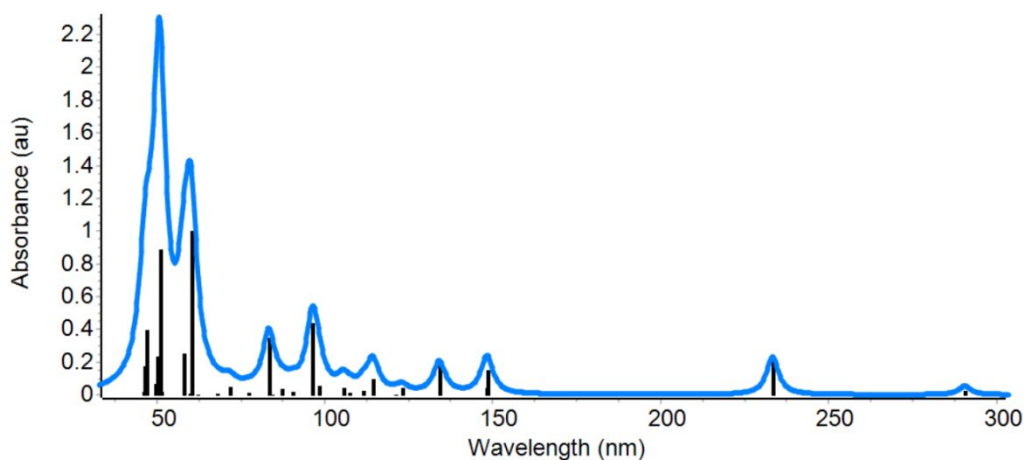


Fig 4. TD-DFT calculated absorption spectra for N_3^- .

Table 1. PN yield under no UV light, 254 nm UV light, and 365 nm UV light.

Sample	Nitrogen Desorption Amount (mmol/g)
PN-MWNT	1
PN-MWNT 254 nm	3.9
PN-MWNT 365 nm	0.9

The resulting PN produced from these CV experiments were characterized with Raman and IR spectroscopy. DFT was also used to predict the Raman and IR spectra of each PN molecule; the peaks computed for the N₈ with a zigzag ZEZ configuration match the experimental results, as seen in Fig. 5a and 5b, as well as Table 2. These values are in agreement with the previous work¹⁹: the 2059 cm⁻¹ IR peak matches the 2050 cm⁻¹ experimental peak, and the 1049 cm⁻¹ Raman peak matches the 1080 cm⁻¹ experimental peak. The slight discrepancies could be attributed to solvation and thermal effects that were not included in the model.

Table 2. DFT computed versus experimentally determined Raman and IR major peaks.

	Raman peaks (cm ⁻¹)	IR peaks (cm ⁻¹)
ZEZ DFT	1049	2059
Experiment	1080	2050

These findings present a facile way to synthesize PN under ambient conditions. Conventional PN synthesis has consisted of N₂ precursors, a transformation which has required very high temperatures and pressures. For example, in a 2004 experiment by Eremets *et al.*, the cubic gauche (cg) form of PN was synthesized by laser heating molecular N₂ to a temperature of 2000 K at a pressure of 110 GPa in a diamond cell. In 2007, Gregoryanz *et al.*⁶ raised temperatures to 150 GPa and pressures to 2000 K, for a diamond cell system with N₂ precursors; they were able to construct a phase diagram for various polynitrides. In 2014, Tomasino *et al.*⁷ also used a diamond anvil system with N₂ precursors, at pressures between 120 and 180 GPa and temperatures up to 3000 K, to produce the Pba2 phase of PN. Because of the very high energy barriers associated with breaking the bonds of N₂ to form single bonds in PN, these N₂ precursor methods require extreme conditions. A DFT study by Plašienka *et al.*³⁰ articulates the synthesis mechanism for

transforming N_2 to cg PN at high temperature and pressure conditions, and found that it proceeds through a number of intermediate crystal structures only possible at high pressure.

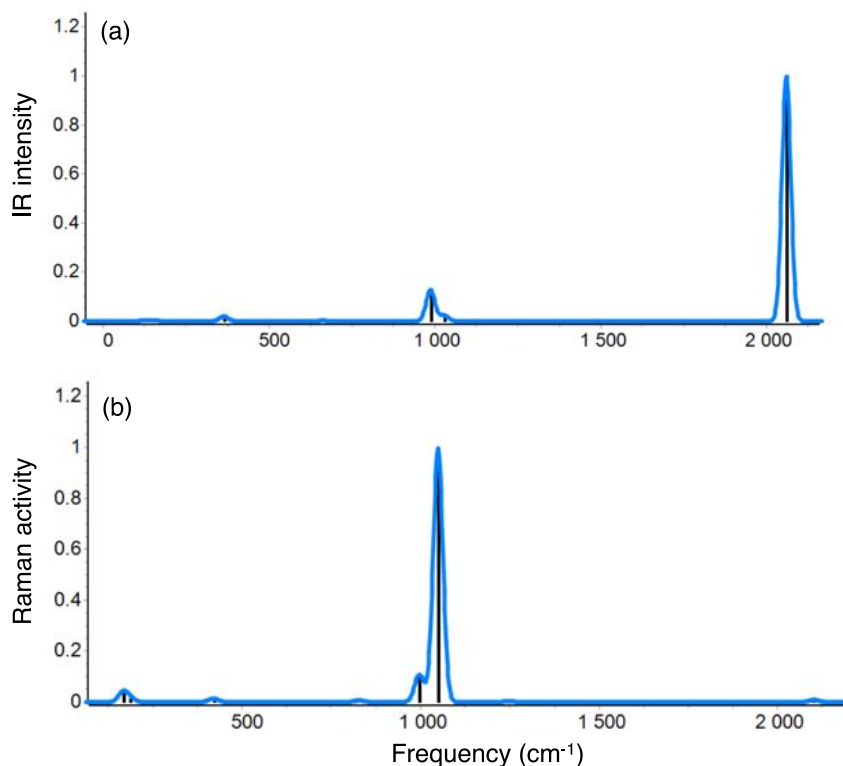


Fig 5. DFT calculated IR and Raman spectra for N_8^- .

In contrast, this study presents the synthesis of PN from an azide precursor, at ambient conditions. By explicating the synthesis mechanism in vacuum, this study shows the plausibility of producing PN with significantly less energy requirements. In fact, this synthesis mechanism has been shown to consist of several spontaneous and low activation energy steps, highlighting the facile nature of this synthesis method. Moreover, this synthesis mechanism indicates that whereas other PN stabilization methods have often involved substrate effects,^{2,8,10} the interactions of N_3 , N_6 , N_{12} and N_{10} isomers lead to the formation of N_8 without the need of a substrate. As the highest barrier of the chemical process from N_3^* to N_8^- is the 20 kcal/mol barrier between N_6 and N_{12} , the barriers are low enough to be overcome by CV methods.

In addition to the contrast with conventional, energy-intensive methods, the synthesis mechanism here underpins the ease with which the yield can be enhanced through UV light exposure. While there has not been much information in published literature on increasing PN

yield, it can be surmised that conventional synthesis methods would improve yield only with great difficulty, due to the high energy required in N_2 diamond anvil cell transformations. This study, on the other hand, demonstrates that yield can be enhanced in a simple and practical way. This UV light technique for enhancement adds to the appeal of the PN, which has been shown to rival platinum in ORR activity.¹⁹ PN is thus promising not only as a high energy-density material with excellent catalytic ability, but as a material that can be synthesized in a facile and scalable way, with a new mechanistic understanding of synthesis at ambient conditions.

4. Conclusion

Using *ab initio* calculations, a practical and rational way to produce N_8^- PN from N_3^- is determined. The detailed mechanism is an intuitive and logical process of dissociating N_2 pairs from the endpoints of N_{12} chains formed from N_6 , which is in turn spontaneously formed from N_3 radicals. This study also explicates the energy barriers for each state, by calculating the saddlepoint optimizations, and for the last ionization step, an NEB value. The stability of each state was confirmed and transition states were determined through vibrational frequency calculations. It was found that the radicalization of azide N_3^- is the rate limiting step. A TD-DFT calculation was used to calculate the absorption spectrum of N_3^- and predict a method of yield enhancement via illumination under UV light. An experiment confirmed this enhancement by a generating yield four times greater than without illumination. This understanding of the PN synthesis and approach to yield enhancement can be utilized to scale up production of this excellent catalytic material in applications such as fuel cells, where the PN can act as a cathodic catalyst. In the future, the effect of the different substrates on the N_8 yield will be elucidated.

Acknowledgements:

This work was supported by NSF CBET-1804949. Density functional theory calculations were performed using high performance computing clusters at the New Jersey Institute of Technology (“Kong” and “Lochness”).

Contributions:

S. Alzaim did the theoretical calculation and wrote the manuscript. Z. Wu did UV irradiation experiments. M. Benchafia helped S. Alzaim with initial FTIR and Raman calculation methods. J. Young guided S. Alzaim with different DFT methods. X. Wang supervised the students and led the research project. Both J. Young and X. Wang finalized the manuscript.

References:

- 1 Y. Li, X. Feng, H. Liu, J. Hao, S. A. T. Redfern, W. Lei, D. Liu and Y. Ma, Route to high-energy density polymeric nitrogen t-N via He-N compounds, *Nat. Commun.*, 2018, **9**, 1–7.
- 2 S. Niu, S. Liu, B. Liu, X. Shi, S. Liu, R. Liu, M. Yao, T. Cui and B. Liu, High energetic polymeric nitrogen sheet confined in a graphene matrix, *RSC Adv.*, 2018, **8**, 30912–30918.
- 3 Y. Li, H. Bai, F. Lin and Y. Huang, Energetics and electronic structures of nitrogen chains encapsulated in zigzag carbon nanotube, *Phys. E Low-Dimensional Syst. Nanostructures*, 2018, **103**, 444–451.
- 4 X. Li, *Principles of fuel cells*, CRC Press, 2005.
- 5 M. I. Eremets, A. G. Gavriliuk, I. A. Trojan, D. A. Dzivenko and R. Boehler, Single-bonded cubic form of nitrogen, *Nat. Mater.*, 2004, **3**, 558–563.
- 6 E. Gregoryanz, A. F. Goncharov, C. Sanloup, M. Somayazulu, H. K. Mao and R. J. Hemley, High P-T transformations of nitrogen to 170 GPa, *J. Chem. Phys.*, , DOI:10.1063/1.2723069.
- 7 D. Tomasino, M. Kim, J. Smith and C. S. Yoo, Pressure-induced symmetry-lowering transition in dense nitrogen to layered polymeric nitrogen (LP-N) with colossal raman intensity, *Phys. Rev. Lett.*, 2014, **113**, 1–5.
- 8 H. Abou-Rachid, A. Hu, V. Timoshevskii, Y. Song and L. S. Lussier, Nanoscale high energetic materials: A polymeric nitrogen chain N₈ confined inside a carbon nanotube, *Phys. Rev. Lett.*, 2008, **100**, 1–4.
- 9 W. Ji, V. Timoshevskii, H. Guo, H. Abou-Rachid and L. Lussier, Thermal stability and formation barrier of a high-energetic material N₈ polymer nitrogen encapsulated in (5,5) carbon nanotube, *Appl. Phys. Lett.*, 2009, **95**, 10–13.
- 10 V. Timoshevskii, W. Ji, H. Abou-Rachid, L. S. Lussier and H. Guo, Polymeric nitrogen in a graphene matrix: An ab initio study, *Phys. Rev. B - Condens. Matter Mater. Phys.*, 2009, **80**, 1–5.
- 11 B. Hirshberg, R. B. Gerber and A. I. Krylov, Calculations predict a stable molecular crystal of N₈, *Nat. Chem.*, 2014, **6**, 52–56.
- 12 S. Battaglia, S. Evangelisti, T. Leininger and N. Faginas-Lago, in *International Conference on Computational Science and Its Applications*, 2018, pp. 579–592.

- 13 R. J. Bartlett, Structure and Stability of Polynitrogen Molecules and their Spectroscopic Characteristics, 2002, **8435**, 1–93.
- 14 F. Barat, B. Hickel and J. Sutton, Flash photolysis of aqueous solutions of azide and nitrate ions, *J. Chem. Soc. D Chem. Commun.*, 1969, 125b--126.
- 15 A. Treinin and E. Hayon, Spectroscopic observation of the azide radical in solution, *J. Chem. Phys.*, 1969, **50**, 538–539.
- 16 E. Hayon and M. Simic, Absorption spectra and kinetics of the intermediate produced from the decay of azide radicals, *J. Am. Chem. Soc.*, 1970, **92**, 7486–7487.
- 17 S. M. Peiris and T. P. Russell, Photolysis of compressed sodium azide (NaN₃) as a synthetic pathway to nitrogen materials, *J. Phys. Chem. A*, 2003, **107**, 944–947.
- 18 N. Holtgrewe, S. S. Lobanov, M. F. Mahmood and A. F. Goncharov, Photochemistry within compressed sodium azide, *J. Phys. Chem. C*, 2016, **120**, 28176–28185.
- 19 Z. Wu, E. M. Benchafia, Z. Iqbal and X. Wang, N₈ polynitrogen stabilized on multi-wall carbon nanotubes for oxygen-reduction reactions at ambient conditions, *Angew. Chemie - Int. Ed.*, 2014, **53**, 12555–12559.
- 20 F. Neese, Software update: the ORCA program system, version 4.0, *Wiley Interdiscip. Rev. Comput. Mol. Sci.*, 2018, **8**, e1327.
- 21 A. Schäfer, H. Horn and R. Ahlrichs, Fully optimized contracted Gaussian basis sets for atoms Li to Kr, *J. Chem. Phys.*, 1992, **97**, 2571–2577.
- 22 T. H. Dunning Jr, Gaussian basis sets for use in correlated molecular calculations. I. The atoms boron through neon and hydrogen, *J. Chem. Phys.*, 1989, **90**, 1007–1023.
- 23 A. D. Becke, Becke's three parameter hybrid method using the LYP correlation functional, *J. Chem. Phys.*, 1993, **98**, 5648–5652.
- 24 S. Haldar, C. Riplinger, B. Demoulin, F. Neese, R. Izsak and A. K. Dutta, Multilayer approach to the IP-EOM-DLPNO-CCSD method: Theory, implementation, and application, *J. Chem. Theory Comput.*, 2019, **15**, 2265–2277.
- 25 S. Grimme, J. Antony, S. Ehrlich and H. Krieg, A consistent and accurate ab initio parametrization of density functional dispersion correction (DFT-D) for the 94 elements H–Pu, *J. Chem. Phys.*, 2010, **132**, 154104.
- 26 J. Jenke, A. N. Ladines, T. Hammerschmidt, D. G. Pettifor and R. Drautz, Tight-binding bond parameters for dimers across the periodic table from density-functional theory, 2019,

- 1–12.
- 27 S. Grimme, Exploration of Chemical Compound, Conformer, and Reaction Space with Meta-Dynamics Simulations Based on Tight-Binding Quantum Chemical Calculations, *J. Chem. Theory Comput.*, 2019, **15**, 2847–2862.
- 28 G. A. Zhurko, 2019.
- 29 M. J. Greschner, M. Zhang, A. Majumdar, H. Liu, F. Peng, J. S. Tse and Y. Yao, A New Allotrope of Nitrogen as High-Energy Density Material, *J. Phys. Chem. A*, 2016, **120**, 2920–2925.
- 30 D. Plašienka and R. Martoňák, Transformation pathways in high-pressure solid nitrogen: From molecular N₂ to polymeric cg-N, *J. Chem. Phys.*, 2015, **142**, 1–10.